Freeman, Tom C. A., Haynes, Joshua D., Gallagher, Maria and Culling, John F. (2026) *On manipulating motion gain in immersive virtual environments: An unidentified source of external noise and a new psychometric function.* Journal of Vision, 26 (6). ISSN 1534-7362.

On manipulating motion gain in immersive virtual environments: An unidentified source of external noise and a new psychometric function

Tom C. A. Freeman School of Psychology, Cardiff University, Cardiff, UK

Joshua D. Haynes School of Health Sciences, University of Manchester, Manchester, UK

Maria Gallagher School of Psychology, Keynes College, University of Kent, Kent, UK

John F. Culling School of Psychology, Cardiff University, Cardiff, UK

In immersive virtual environments and other interactive settings the motion gain linking stimulus motion to self-movement is often manipulated to study perceptual performance. We show that this introduces a previously unidentified source of external noise we term *gain-dependent noise*. The noise arises from trial-to-trial variability in self-movement and can distort the shape of the psychometric function. This leads to overestimates of threshold and sensory measurement noise, and misinterpreted lapse rates when fitting standard sigmoidal functions like a cumulative Gaussian. Using a model observer with minimal assumptions, simulations show the situation is more critical when the coefficient of variation of self-movement (i.e., across-trial standard deviation/mean) is relatively high, and measurement noise associated with image-based and idiothetic signals is relatively low. We derive a new gain-dependent psychometric function that separates sensory measurement noise from gain-dependent noise, and provide a MATLAB fitting routine (*fitgdpmf*).

Introduction

A common way to assess the perception of movement in immersive visual environments (IVEs) is to manipulate the natural relationship between self-movement and image motion in a head-mounted display (HMD) or equivalent (Chen, Ladeveze, Hu, Ou, & Bourdot, 2019; Dyde & Harris, 2008; Gallagher, Haynes, Culling, & Freeman, 2025; Grechkin, Thomas, Azmandian, Bolas, & Suma, 2016; Halow, Liu, Folmer, & MacNeilage, 2023; Haynes, Gallagher, Culling, & Freeman, 2024; Jaekl, Jenkin, & Harris, 2005; Kruse, Langbehn, & Steinicke, 2018; Moroz, Garzorz, Folmer, & MacNeilage, 2019; Steinicke, Bruder, Jerald, Frenz, & Lappe, 2008; Steinicke, Bruder, Jerald, Frenz, & Lappe, 2009; Teng, Allison, & Wilcox, 2023; Williams & Peck, 2019). For instance, Steinicke and colleagues asked observers to detect increases and decreases in the expected magnitude of image movement when walking or rotating their head and found they did so relatively poorly. Most often it is visual performance under investigation, but the technique can been extended to hearing (Nilsson, Suma, Nordahl, Bolas, & Serafin, 2016; Serafin, Nilsson, Sikstrom, De Goetzen, & Nordahl, 2013). The manipulation of motion gain also drives redirected walking (Fan, Li, & Shi, 2022; Nilsson et al., 2018; Razzaque, Swapp, Slater, Whitton, & Steed, 2002), where users navigating large virtual terrains are nudged to walk differently within confined physical spaces by using subtle changes to the ongoing image movement.

The technique alters a multiplicative gain term (g) linking the position of the scene's image within the display (I) to real-time measurements of head position (H):

$$\mathrm{I}(t) = -g\mathrm{H}(t) \quad (1)$$

In general, I and H are vectors specifying translation and rotation. Motion gain can therefore be manipulated along all or a subset of dimensions (Steinicke et al., 2008). For a head rotation about a vertical yaw axis, $g = 1$ produces a world-stationary scene rotating equal and

Citation: Freeman, T. C. A., Haynes, J. D., Gallagher, M., & Culling, J. F. (2026). On manipulating motion gain in immersive virtual environments: An unidentified source of external noise and a new psychometric function. *Journal of Vision*, *26*(6):9, 1–15, https://doi.org/10.1167/jov.26.6.9.

https://doi.org/10.1167/jov.26.6.9 Received August 13, 2025; published June 25, 2026 ISSN 1534-7362 Copyright 2026 The Authors

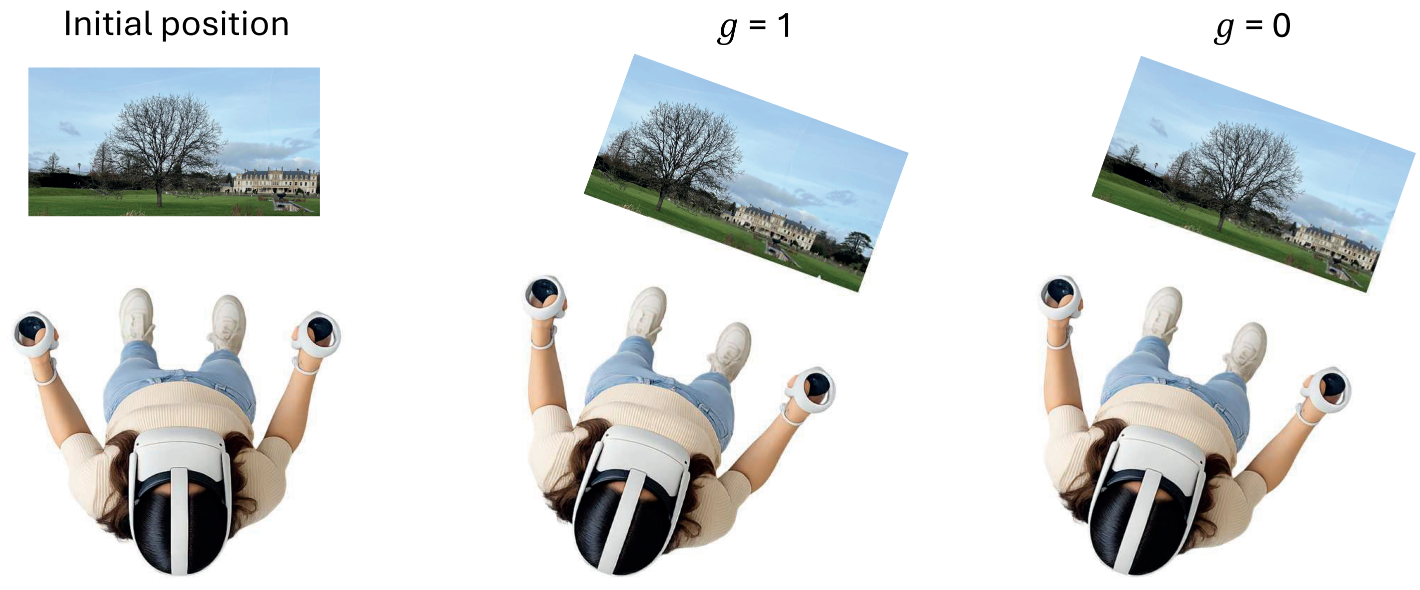

Figure 1. Illustration of the relationship between motion gain, image motion and head movement. The result of applying a gain of 1 and 0 from an initial front-forward position (*left*) are shown *middle* and *right*, respectively. Some parts of the figure were generated using ChatGPT.

opposite to the head movement in the display (compare left and middle panels in Figure 1). On the other hand, if $g = 0$, the scene remains stationary in the display and so moves with the observer (compare left and right panels in Figure 1). Motion gain can be made to take on any value, which allows the experimenter to investigate the psychophysical relationship between self-movement and display motion. For instance, Steinicke et al. (2008), Steinicke et al. (2009) fit psychometric functions to the probability of observers choosing whether the physical self-movement was greater than the virtual movement in the HMD; while we and others have used the probability of choosing whether the display appeared to move left versus right, or "with" and "against," during horizontal head rotation (Gallagher et al., 2025; Halow, Hamilton, Folmer, & MacNeilage, 2023; Halow, Liu, et al., 2023; Haynes et al., 2024).

The psychometric function reveals two important aspects of the observer. The first is their perceptual bias, which in motion-gain experiments is determined by the gain needed to make stimuli appear stationary in the (virtual) world. This is commonly referred to as the Point of Subjective Equality (PSE). The PSE will be at $g = 1$ if the neural system comparing display motion to self-movement worked perfectly. However, the PSE often lies within the range $0 < g < 1$ (Dyde & Harris, 2008; Gallagher et al., 2025; Halow, Liu, et al., 2023). This indicates that neural estimates of display motion in the IVE are larger than corresponding idiothetic cues to self-movement from vestibular and motor systems. The second aspect revealed by the psychometric function is the observer's precision, often termed their threshold. This corresponds to the slope of the psychometric function, and is typically used to estimate noise within the biological system. The threshold in motion-gain experiments is most likely determined by noise associated with neural estimates of image motion and idiothetic cues. We call this "measurement noise" and note that it is driven by both internal variability and external uncertainty. The latter can be manipulated in a number of different ways, such as changing visual contrast (Champion & Warren, 2017; Powell, Meredith, McMillin, & Freeman, 2016; Sotiropoulos, Seitz, & Seriés, 2014; Stocker & Simoncelli, 2006; Thompson, 1982), embedding target sounds in background noise (Kerber & Seeber, 2012), or walking on springy surfaces (MacLellan & Patla, 2006). But as we show below, experiments manipulating motion gain contain an additional source of "gain-dependent" noise that has largely been overlooked. Crucially, this source of noise can influence the shape of the psychometric function, and therefore the interpretation of thresholds and estimates of measurement noise.

We have recently proposed a new type of psychometric function (Haynes et al., 2024) that allows the experimenter to separate estimates of measurement noise from gain-dependent noise. Here, we explore the consequences of ignoring gain-dependent noise in more detail. In anticipation, our simulations reveal two types of problem. First, when self-movement has a high coefficient of variation (i.e., across-trial standard deviation/mean), gain-dependent noise causes the psychometric function to differ in shape from a standard sigmoid typically fit to the data (e.g., a cumulative Gaussian). This can lead to large overestimates of measurement noise, along with potential misinterpretation of asymptotic performance when a lapse rate parameter is included in the fit. Secondly, when the coefficient of variation (CV) is low, allowing a standard sigmoid to fit the data well, measurement noise cannot be read directly from the psychometric function. Both cases lead to important consequences in interpreting perceptual performance in IVEs and beyond. Examples include areas which estimate cue reliability from measurement noise, such as redundant cue combination (Alais & Burr, 2004; Ernst & Banks, 2002; Hillis, Ernst, Banks, & Landy, 2002; Hillis, Watt, Landy, & Banks, 2004; Landy, Maloney, Johnston, & Young, 1995; Oruç, Maloney, & Landy, 2003) or the interaction of Bayesian priors with sensory evidence (Burge, Fowlkes, & Banks, 2010; Freeman, Champion, & Warren, 2010; Garcia, Jones, Rubin, & Nardini, 2017; Girshick, Landy, & Simoncelli, 2011; MacNeilage, Banks, Berger, & Bulthoff, 2007; Mamassian, Landy, & Maloney, 2002; Powell et al., 2016; Sotiropoulos et al., 2014; Stocker & Simoncelli, 2006; Wei & Stocker, 2015). For this reason, we provide a MatLab function *fitgdpmf* that controls for gain-dependent noise when fitting a psychometric function, along with a script *simulationcode* that was used to generate the main results reported below (see Methods for URL).

Gain-dependent psychometric function

Model observer

The psychometric function is a model of observer performance—it makes assumptions about the information available, the decisions made by the observer and the limits set by measurement noise. In this section, we derive a gain-dependent psychometric function by describing a model observer based on reasonable assumptions about the nature of measurement noise, how internal estimates of self-movement and display motion are combined, and how psychophysical decisions are made.

Suppose the task for a moving observer is to judge the direction of virtual movement for a particular set of motion gains defined by a Method of Constant Stimuli. For simplicity, we assume that trials are relatively short, containing brief segments of continuous head-movement in one direction, with the display consisting of a single object or a scene that is visual, auditory or both. Under these constraints, the psychophysical judgements reduce to simple binary decisions, like did the display appear to move left versus right as the head rotated, or "too much" versus "too little" as they walked (we generalize to extended sequences, less constrained self-movement, and different types of judgement later).

In general, the real-world motion (M) of an object or scene is the sum of head movement (H) and the audiovisual image motion in the HMD (I):

$$M = I + H \quad (2)$$

where I and H correspond to the derivatives of I and H in Equation 1 with respect to time. To estimate M, the observer must measure I and H from internal signals i and h. For vision, matters are made more complicated than hearing because the eyes move: motion in the retinal image is therefore different from the motion in the HMD, a point discussed later. We make no assumptions about how the observer arrives at the estimates of i and h: these could be based on average speed or displacement, a peak value, or some other metric, so long as they yield a single point estimate on each trial, and as long as the observer adheres to the same measure. Across trials, i and h are corrupted by measurement noise:

$$i = \mu_i + \varepsilon_i \quad (3)$$

$$h = \mu_h + \varepsilon_h \quad (4)$$

where ε_i and ε_h are error terms drawn from a Gaussian distribution i.e. $\varepsilon \sim \mathcal{N}(0, \sigma^2)$. Head movement H will also vary stochastically across trials, which means h must vary too. The mean μ_h is therefore also a random variable. This will be the case for μ_i as well, because image motion and head movement are linked via motion gain, as defined by Equation 1. Assuming H is Gaussian distributed (see example in Haynes et al., 2024):

$$i = -g\,(\mu_H + \varepsilon_H) + \varepsilon_i \quad (5)$$

$$h = b\,(\mu_H + \varepsilon_H) + \varepsilon_h \quad (6)$$

where b is a linear bias term that defines the accuracy of the head-movement signal relative to its input, such that the expectation $E(h) = E(bH)$. The bias term captures known differences in accuracy between head movement signals and image-movement signals[1]. Examples include the findings that stationary sound sources appear to move slightly against the head rotation (Freeman, Culling, Akeroyd, & Brimijoin, 2017), and visual stimuli appear slower when tracked by a whole-body rotation (Garzorz, Freeman, Ernst, & MacNeilage, 2018). Both findings imply $b < 1$, analogous to equivalent perceptual biases that occur in motion perception during smooth pursuit (Freeman, 2001; Freeman & Banks, 1998; Freeman, Banks, & Crowell, 2000; Furman & Gur, 2012; Souman, Hooge, & Wertheim, 2006; Wertheim, 1994; Xu & DeAngelis, 2025).

Substituting (5) and (6) into (2), perceived motion (m) is therefore given by:

$$m = \ (b - g)\,(\mu_H + \varepsilon_H) + \varepsilon_h + \varepsilon_i \quad (7)$$

Psychometric function

In the proposed experiment, motion gain is varied across trials and observers make a binary decision about the direction of m based on its sign (e.g. the scene appeared to move to the left or right). The collection of responses across multiple trials therefore describes the probability of judgements in a particular direction as a function of g. Following standard signal detection theory (e.g. Jones, 2016), m forms a decision variable:

$$d' = \frac{\mu_m}{\sigma_m} \quad (8)$$

where, by inspecting Equation 7:

$$\mu_m = (b - g)\,\mu_H \quad (9)$$

Equation (7) also determines the standard deviation via the variances-sum law for Gaussian distributions:

$$\sigma_m = \sqrt{(b-g)^2\sigma_H^2 + \sigma_h^2 + \sigma_i^2} \quad (10)$$

The probability of choosing one of two directions is given by:

$$P = \frac{\lambda}{2} + (1 - \lambda)\,\Phi\left(d'\right) \quad (11)$$

where λ is the lapse rate and Φ is the cumulative distribution function of the standard normal distribution:

$$\Phi\,(\mathrm{z}) = \frac{1}{\sqrt{2\pi}} \int_{-\infty}^{z} e^{-z^2}/2\,dz \quad (12)$$

Initial observations

Equations 10–12 suggest that fitting a standard sigmoidal function like a cumulative Gaussian will only work when head-movement variability (σ_H^2) is 0. In this case, the total amount of measurement noise can be recovered from the best-fitting cumulative Gaussian, assuming that both noise sources (σ_h and σ_i) are constant across the range of motion gains used to determine the psychometric function (the "fixed noise" assumption: Georgeson & Meese, 2006). But when $\sigma_H^2 \neq 0$, variable head movement makes recovery of measurement noise more complicated because it produces an additional source of gain-dependent noise via the term $(b - g)^2\sigma_H^2$.

The effect is demonstrated in Figures 2A and 2B. The same gain-dependent psychometric functions have been generated by finely sampling the motion gain axis, with the model observer assumed to have a lapse rate of 0 (i.e. $\lambda = 0$). In addition to the motion gain (g) defined above, the psychometric functions are also plot against "world" gain (g_w) for reasons discussed in the Methods section. The red curves plot the best-fitting cumulative Gaussian, obtained using the Palamedes toolbox (Prins & Kingdom, 2018), with an arbitrarily large number of trials assumed at each gain value (see Methods for details). For Figure 2A, the fit assumes a fixed lapse rate of 0, the same as the model observer. For Figure 2B, the lapse rate was free to vary. Although the PSE is unaffected, the cumulative Gaussian clearly does not fit well in either case. The fit improves when lapse rate is free, but being right for the wrong reasons is seldom a good policy. In the case shown, the best-fitting lapse rate is 0.05, some margin from the actual lapse rate of 0 that was built into the model observer.

Figures 2A and 2B demonstrate two important effects of gain-dependent noise: (1) the asymptotes of the psychometric function move away from $P = (0, 1)$, mimicking the effect of a non-zero lapse rate; (2) the best-fitting cumulative Gaussian has a shallower slope when the correct lapse rate is assumed, overestimating threshold. The reason for the asymptotic behavior is illustrated in Figure 2C. Each panel shows the distributions of the decision variable (d') for five motion gains centered either side of the PSE (i.e., $d' = 0$), and a given amount of head movement variability (σ_H^2). When $\sigma_H^2 = 0$ (top panel), the spread of the decision distributions consists of measurement noise alone. The distributions shift to the right as motion gain increases; hence the probability P of choosing one of the two response categories corresponds to the area under the curve to the right of $d' = 0$. Because we assume fixed measurement noise, each of these areas define different points along a single cumulative Gaussian. However, as head movement variability increases from 0 (lower three panels), the spread depends on the additional gain-dependent noise. The spread changes with gain, emphasizing why standard sigmoidal functions like a cumulative Gaussian cannot fit the data. Moreover, the area under the curve to the right of $d' = 0$ converges on a fixed, non-zero proportion of the total as motion gain moves to ever larger values either side of the PSE. The asymptotes of the psychometric function must therefore move away from $P = (0, 1)$. Gain-dependent noise becomes confounded with lapse-rate.

Figure 2 suggests the degree to which gain-dependent noise causes substantial departures from a cumulative Gaussian depends on a number of factors. These include the kinematics of self-movement (i.e., its mean and across-trial variability), the underlying

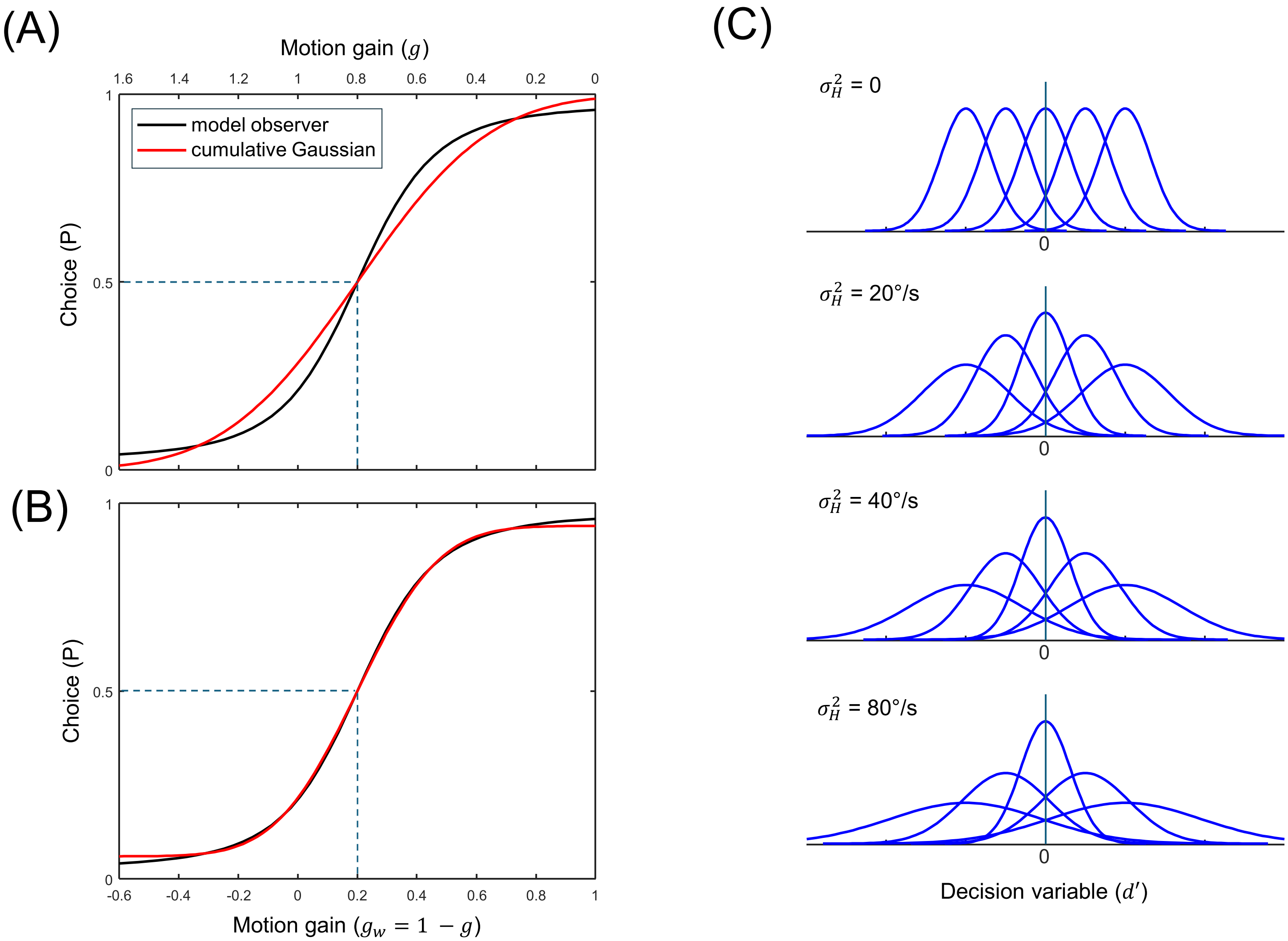

Figure 2. (**A**) The black curve shows a psychometric function based on a model observer with gain-dependent noise with $\{\mu_H,\ \sigma_H,\ (\sigma_i^2+\sigma_h^2)^{1/2},\ \ b,\ \ \lambda\} = \{40,\ 20,\ 9.14,\ 0.8,\ 0\}$. The red curve is the best fitting cumulative Gaussian as determined by the Palamedes toolbox, again with $\lambda = 0$. (**B**) This time the lapse-rate was free to vary, with the best-fitting value found to be 0.05. The result is near perfect, emphasizing how lapse-rate and gain-dependent noise can be confounded. (**C**) Probability distributions of d′ for five different levels of motion gain. Each panel shows a different level of head movement variability: when greater than 0, the d′ distribution becomes "gain dependent." The standard deviation of the set of Gaussians depends on the distance from the PSE. Moreover, there is always a significant proportion of the area under the curve that crosses the decision boundary $d' = 0$. This is the reason that the tails of the psychometric functions generated by the model observer compress.

measurement noise and whether lapse-rate is allowed to vary in the fit. The impact of these factors will also depend on the way the experimenter measures psychophysical performance. Unlike Figure 2, real experiments use a relatively small number of trials based on a few motion gains repeated a handful of times. We therefore carried out a number of simulations that placed the model observer and the fitting of a standard sigmoid in a more realistic setting. This included defining a realistic kinematic space spanned by self-movement mean and variability, one that researchers are more likely to confront when testing human participants.

Methods

Overview

The model observer is parameterised by $\theta = \{\mu_H,\ \sigma_H,\ (\sigma_i^2+\sigma_h^2)^{1/2},\ \ b,\ \ \lambda\}$. In the simulations, we set $b = 1$ and $\lambda = 0$, and used a specific regime described below to define the accompanying measurement noise $(\sigma_i^2+\sigma_h^2)^{1/2}$. To evaluate how well a cumulative Gaussian describes the gain-dependent psychometric function, and its effect on parameter estimates, we followed the approach of Scarfe (2022).

We ran 100 experiments for every (μ_H, σ_H) sampled in the two-dimensional "kinematic" space. For each experiment, a cumulative Gaussian was fit to a new set of model observer responses generated by θ, using motion gain values defined by a Method of Constant Stimuli typical of the area (10 trials at nine linearly-spaced steps spanning a gain range $\pm$ 0.5 about the PSE). We evaluated the effect of gain-dependent noise by assessing goodness-of-fit and the estimate of measurement noise. Goodness-of-fit was determined by a bootstrapping procedure described below, which yielded the percentage of experiments deemed "safe" in a statistical sense. The estimate of measurement noise was evaluated by comparing the ratio of slopes of the two functions at the PSE. The goodness-of-fit measurement therefore assesses how confident an experimenter would be of each simulated result, while the slope ratio indicates whether that confidence was justified.

The main results consist of four simulations comprising two different levels of measurement noise crossed with a fixed or free lapse rate parameter. When fixed, lapse rate was set to 0, the same value built-in to the model observer and assumed by many of the studies in this area. When free to vary, lapse rate was constrained to lie within the range 0–0.06, as suggested by Wichmann & Hill (2001). We ran a further set of simulations to investigate issues concerning low numbers of trials per stimulus level. The simulation code can be found in the MatLab source file *simulationcode* (see below for URL).

Fitting procedure

We used the function *PAL_PFML_Fit* from the Palamedes toolbox (Prins & Kingdom, 2018) to find the cumulative Gaussian that best fit the responses of the model observer. The cumulative Gaussian was parameterised by two free parameters α, β, corresponding to the position (i.e., PSE) and slope (i.e., threshold) of the psychometric function, and a fixed or free lapse rate that set the upper and lower asymptotes γ and λ (i.e., $\gamma = \lambda$). The best fit was determined using a search grid containing a linear range of α values, a logarithmic range of β values, and a linear range of lapse rates when this parameter was free to vary.

Evaluating goodness-of-fit and estimated measurement noise

The goodness-of-fit between the fitted psychometric functions and the true function generated by the model observer was assessed using a parametric bootstrapping technique performed by *PAL_PFML_GoodnessOfFit*, also from the Palamedes toolbox (Prins & Kingdom, 2018). The technique consists of fitting cumulative Gaussians to a series of simulated datasets generated from the single best-fitting psychometric function determined by *PAL_PFML_Fit*. The bootstrap was based on 200 iterations, each culminating in a deviance measure that compares the log likelihood of the best fit to the log likelihood of the simulated data. The subsequent distribution of deviances can then be used to assess how well the original best fit describes the responses of the model observer: specifically, if the proportion of bootstrapped deviances greater than the deviance of the original fit exceeds 0.95, there is no evidence to reject the fit. From this we calculated the percentage of good fitting experiments at each point in the kinematic space, making sure we screened out bootstrap iterations that led to invalid fits (e.g., infinite slopes as discussed by Prins, 2019).

The kinematic space described in the next section was sampled with a granularity of 21 $\times$ 21 head-movement means and standard deviations. Hence the percentage of good-fitting experiments was determined by almost 9 million fits (441 kinematic samples x 100 experiments x 200 bootstraps). Alongside these we also estimated the best-fitting values of the free parameters. This was done by calculating their mean across the 100 experiments at each point sampled.

We also evaluated how well a best-fitting cumulative Gaussian can estimate the true measurement noise within the model observer, irrespective of how well the cumulative Gaussian fits. The analysis is based on the slopes of the two different psychometric functions at the PSE (see Appendix for derivation). These can then be used to convert best-fitting values of β into an estimate of the true measurement noise. In the Results, we report the ratio of true noise to estimated noise. As we remark in the Appendix, this is almost the same as evaluating the ratio of slopes; the only difference is that the latter scales the ratio of noises by the ratio of lapse rates. Given this close correlation, it is worth noting that a noise ratio $<$ 1 corresponds to an over-estimate of threshold when fitting a cumulative Gaussian.

Kinematic space

Apart from our own, none of the other psychophysical studies cited in this paper report self-movement variability, and only some report an average (Gallagher et al., 2025; Grechkin et al., 2016; Halow, Liu, et al., 2023; Haynes et al., 2024; Jaekl et al., 2005; Moroz et al., 2019). Hence, it is difficult to know what ranges of head-movement average and variability to investigate. The reasons for the lack of data surround attempts to promote consistent self-movement, include constraints placed on observer self-movement (e.g., using a metronome: Jaekl et al, 2005), self-movement

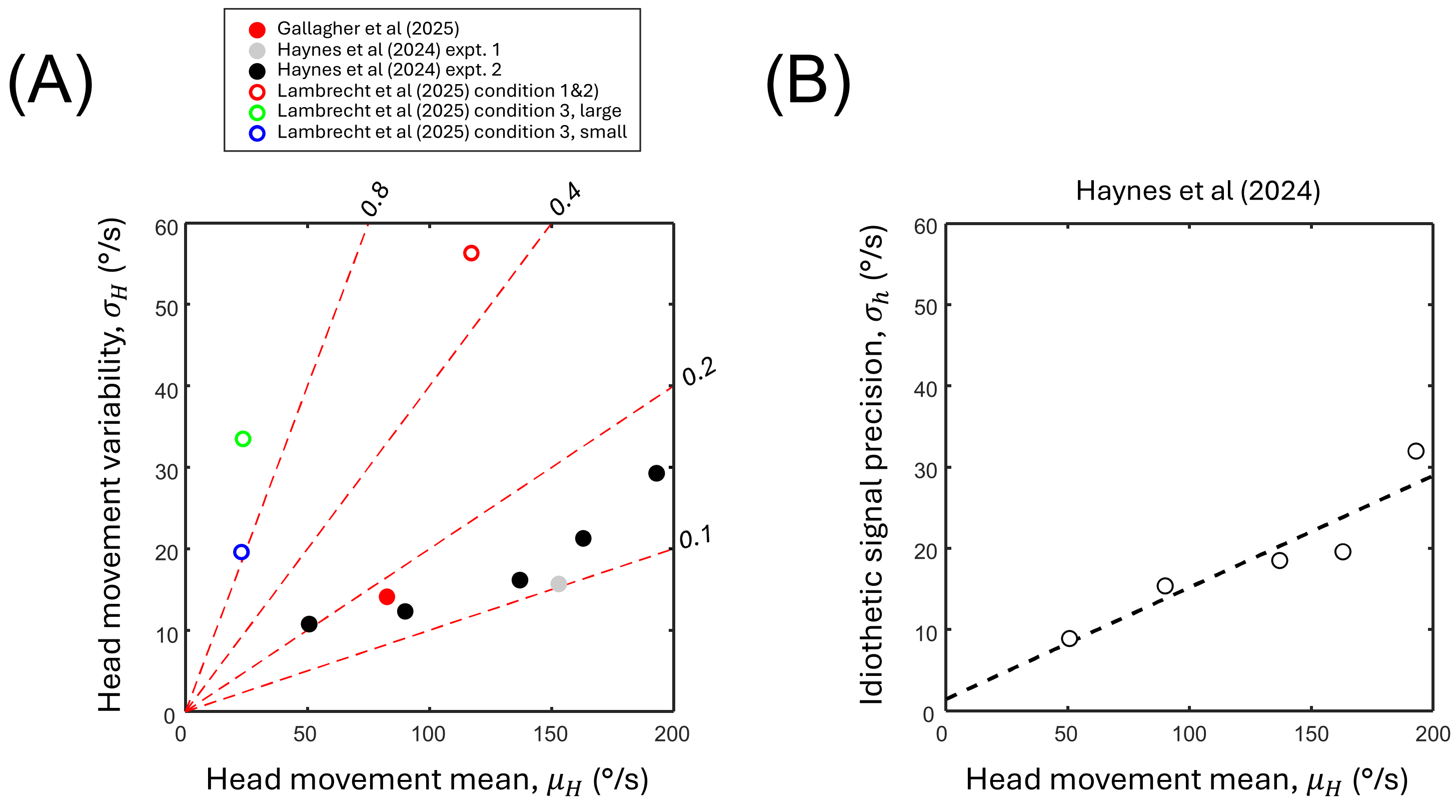

Figure 3. (**A**) Kinematic data from three studies of head rotation. The dashed lines correspond to indicative coefficients of variation (values given around the edge). (**B**) First order polynomial fit to the data of Haynes et al. (2024). The polynomial is used to define both the idiothetic and sensory measurement noise embedded in the model observer.

training prior to data collection (Halow et al., 2023; Halow, Liu, et al., 2023; Haynes et al., 2024; Moroz et al., 2019), and the use of exclusion criteria for trials with aberrant self-movement (Moroz et al., 2019). Even our two papers report variability somewhat implicitly, incorporating estimates of σ_H into a model observer similar to the one defined here. We therefore re-analysed our data to obtain better benchmarks for appropriate ranges of head-movement average and variability. The result is shown in Figure 3A (filled data points), with the dashed lines indicating example coefficients of variation (CV).

In our studies, participants made free head rotations while viewing simple stimuli moving across a loudspeaker/LED ring viewed in a dark and sound-treated lab. Moreover, eye movements were inhibited using head-stationary fixation points. To place our data in a more general context, we therefore re-analyzed data kindly provided to us by Lambrecht, Hallemans and co-authors. They investigated cued head rotations while participants walked freely along a walkway in a well-lit laboratory (Lambrecht et al., 2025). In three conditions, participants wore either a headband, or an inactive HMD, or a Hololens2 augmented-reality HMD. Head rotation cued verbally in the first two conditions, or made to follow an augmented-reality target (a hummingbird) in the third. Using their data, we calculated mean head rotation speed for the same portion of the head sweep used in our two articles (20%–60%). To increase the number of trials, we collapsed their conditions 1 and 2 to calculate across-trial standard deviations.

Their results are shown as open symbols in Figure 3. Perhaps unsurprisingly, the head rotations they measured were more variable than ours (higher CV), given that our participants were seated. Moreover, in their condition 3, they found more variability when prompting participants to make large head rotations over 90° versus small head rotations over 45° (compare green and blue open symbols). Based on the kinematics from these studies, our simulations probed the range defined by the axis dimensions of Figure 3A. In the Discussion, we show how the simulations can be generalized to head translation (walking, running, driving, etc.) in a straightforward manner.

Measurement noise

It is well known that thresholds are roughly proportional to stimulus magnitude over a wide range of values (Weber's law: Laming, 2009). We therefore had to make some assumptions about how measurement noise varied with speed. This is straightforward for the idiothetic signal: Weber's law is a good description for the range of head speeds comfortably executed during active and passive head rotation (Haynes et al., 2024; Mallery, Olomu, Uchanski, Militchin, & Hullar, 2010). Hence, the measurement noise associated with the idiothetic signal is proportional to speed. Figure 3B replots the data of Haynes et al. (2024), Experiment 2, with the dotted line showing the best-fitting 1st order polynomial:

$$\sigma_h = p_1\mu_H + p_2 \quad (13)$$

where $p_1 = 0.14$ and $p_2 = 1.4$. We used this polynomial fit in the simulations. As an aside, the data shown in Figure 3B were obtained while judging auditory targets. In principle, the same levels of idiothetic signal precision should be found for visual targets, because the signal in both conditions is based on non-image inputs from vestibular and motor systems. However, as shown in Haynes et al. (2024), σ_h halves when using visual targets. We point the reader to that article for a discussion of possible reasons why.

For image signals, the situation is more complicated because Weber's law breaks down at low speeds (De Bruyn & Orban, 1988). This is likely due to "resting state" noise increasingly dominating motion discrimination thresholds. Weber's law also breaks down at fast speeds for visual stimuli (it is unclear whether this is the case for hearing—Haynes et al., 2024 showed a good fit to Weber's law for all but slow speeds, similar to previous studies on auditory motion: Altman & Viskov, 1977). To simplify matters, we captured the departure at low speeds using the intercept defined by the fitted polynomial, and ignored any departures at faster speeds. Hence, we define the noise associated with the measurement of IVE display motion as:

$$\sigma_i = p_1 v + p_2 \quad (14)$$

where v is display speed, and p_1 and p_2 are set to the same values as Equation 13. At the PSE, $d' = \mu_m = 0$; hence, from Equation 9, the motion gain is equal to the relative bias (b). Thus, from Equation 5, image speed $v = E(i) = E(b\mu_H)$.

According to our model observer, the overall noise associated with the estimate of motion is a combination of gain-dependent noise and sensory measurement noise. As the latter decreases, we'd expect more influence of gain-dependent noise and potentially greater problems in fitting a standard sigmoid. Given our estimate of measurement noise depends on one study only, we also ran simulations where the slope p_1 was halved for both signals. Such a reduction is plausible for situations different from those investigated by Haynes et al. (2024). For instance, in the case of the image-motion signal, measurement noise would be expected to decline if smaller stimuli were used, or a background was visible. These changes may also impact the self-movement signal too, given that a visible background provides the observer with both idiothetic and image-based estimates of self-movement.

IVE gain versus "world" gain

It is customary to have the variable on the abscissa of a psychometric function to positively correlate with P (indeed, the Palamedes toolbox requires the data to be ascending). This proves problematic when using the particular definition of motion gain used in the IVE literature i.e. Equation 1. For instance, if the experiment involved a leftwards head rotation about the yaw axis, stimuli moving rightward in the virtual scene correspond to the range $1 > g > -\infty$; the motion gain parameter initially becomes progressively smaller and then more negative as stimuli move increasingly to the right. A more intuitive result is obtained by plotting P against "world" gain i.e. $g_w = 1 - g$. Positive values of g_w then correspond to the same direction of object movement in the virtual scene. The consequence is to reflect the psychometric function left to right and shift the origin. P then goes from low to high, not high to low (see Gallagher et al., 2025, for the use of g_w, and Steinicke et al, 2009, for the use of g). These two definitions of motion gain are illustrated in Figure 2 above.

Open-source code

The simulation code can be found at the following link: https://osf.io/3j9dt/overview?view_only=ccb3dd10e60e4068bfbfa3017c9aaaa7. A MATLAB function *fitgdpmf* can also be found there, which can be used to fit the new psychometric function to experimental data. The fitting routine allows either definition of motion gain to be used, and also an option to fix the lapse rate or allow it to vary.

Results

Figure 4 shows the result of fitting a single cumulative Gaussian with a fixed lapse rate when measurement noise is high (top row) or low (bottom row). The first column shows the percentage of "good" fits, while the second column shows the noise ratio (true/estimated); the dotted lines indicate representative coefficients of variation (CVs). Clearly the effect of gain-dependent noise is more problematic for high CVs and low measurement noise. Hence there are fewer good fits above the main diagonal, and these correlate with noise ratios substantially less than 1. For low measurement noise, the percentage of good fits can reduce to 60% to

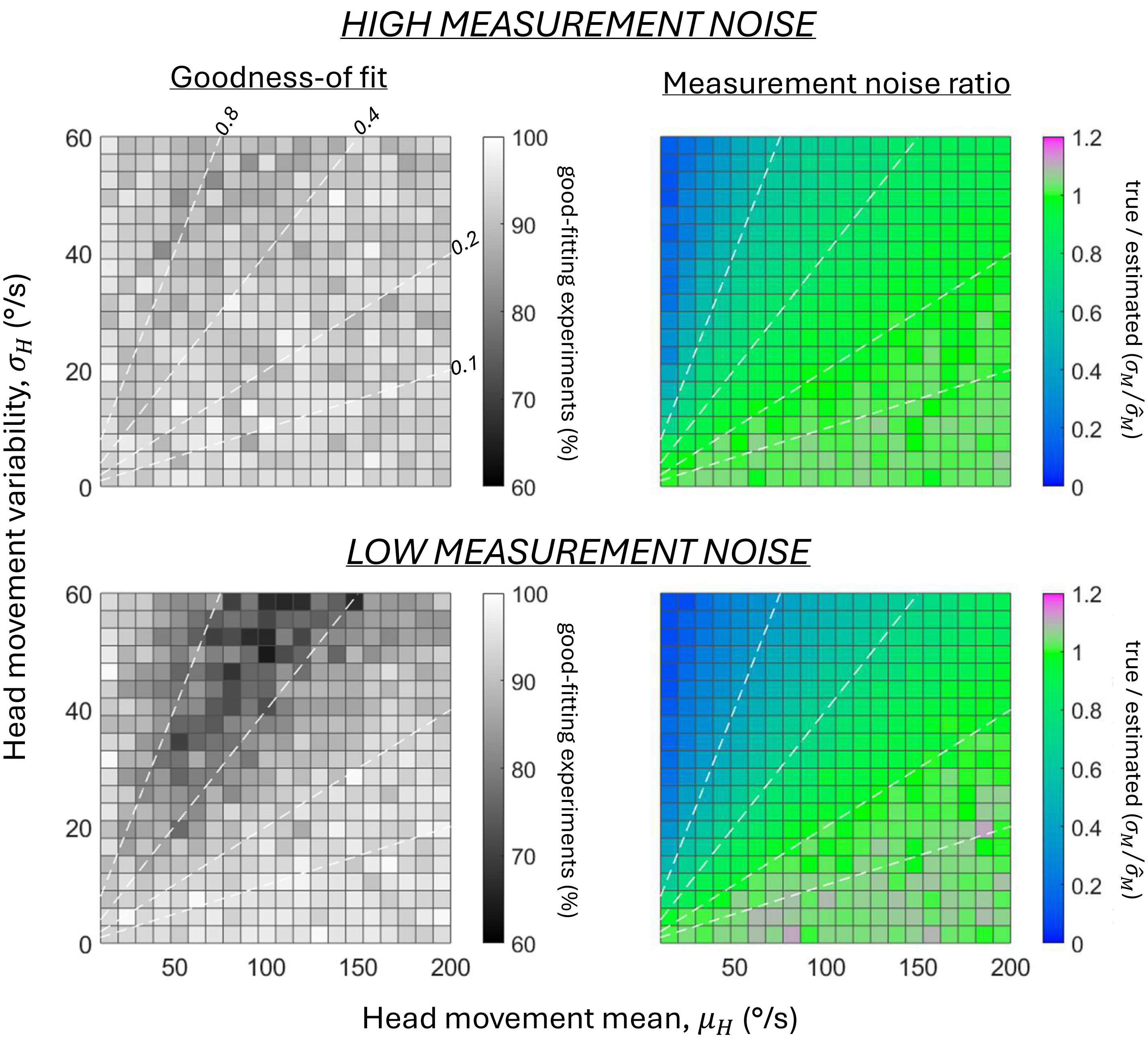

Figure 4. The effects of gain-dependent noise when a cumulative Gaussian with a fixed lapse rate is fit to the model observer. The top row corresponds to the higher level of measurement noise defined by the 1st order polynomial in Figure 3; the bottom row corresponds to lower row noise obtained by halving the slope of that fit. The first column shows the percentage of "good" fits and the second the measurement noise ratio.

70% over a sizeable area of the kinematic space, with noise ratios < 1 occupying substantially more territory too. For large parts of the kinematic space, a cumulative Gaussian therefore overestimates measurement noise, and by the same token, threshold.

Figure 5 shows the same general pattern when lapse rate is free to vary. Although the percentage of good fits is better than the fits achieved with a fixed lapse rate (compare first columns of Figures 4 and 5), the best-fitting lapse rate (final column) is not always correct (recall that the simulations assume a model observer with a lapse rate of 0). Above the main diagonal, the best-fitting lapse rate rises markedly in Figure 5. Indeed, for higher measurement noise, the best-fitting lapse-rate is rarely correct anywhere.

The picture for the noise ratio is more complex. Above the main diagonal, the noise ratio is somewhat closer to 1 when lapse rate is free to vary. Below the main diagonal, however, more instances of noise ratios > 1 occur. Why is this? Both Figures 4 and 5

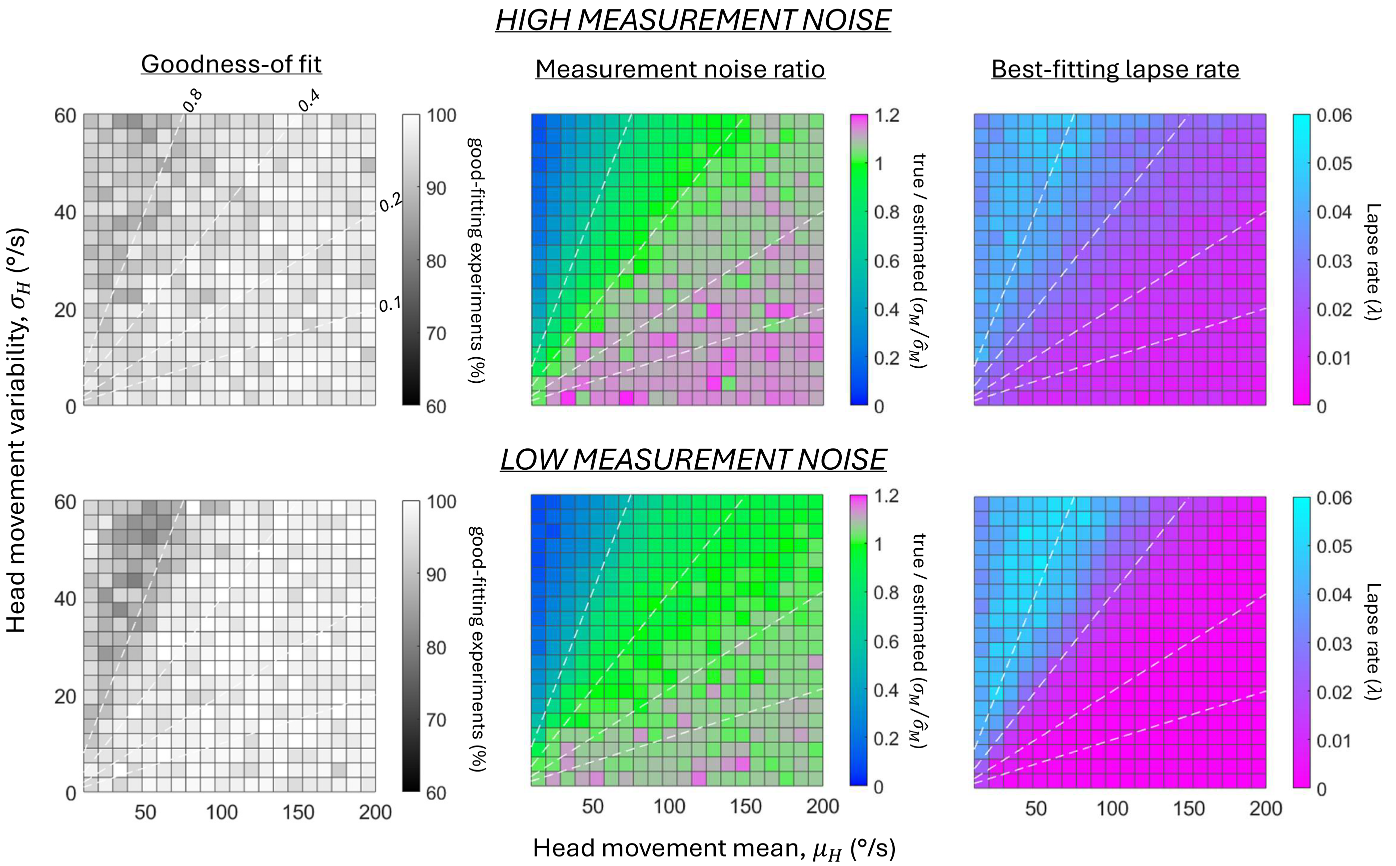

Figure 5. The effects of gain-dependent noise when a cumulative Gaussian with a free lapse rate is fit to the model observer. The top row corresponds to the higher level of measurement noise defined by the first-order polynomial in Figure 3; the bottom row corresponds to lower row noise obtained by halving the slope of that fit. The first column shows the percentage of "good" fits, the second the measurement noise ratio and the third column the best-fitting lapse rate.

show that the overall percentage of good fits increases when sensory measurement noise is high. This makes sense because the psychometric function approaches a cumulative Gaussian as measurement noise increases: in the limit, the fit should be perfect and the noise ratio 1. It is therefore surprising to see this does not happen for low CVs, especially when $\sigma_H = 0$, where there is no gain-dependent noise. This behavior is due to poor sampling of the psychometric function, as opposed to any property of the model observer. Figure 6 shows the result of progressively increasing the number of trials at each stimulus level. For the highest number investigated, noise ratios > 1 all but disappear. This is because larger numbers of trials produce a more highly resolved probability axis, allowing the simulated data sets to take on finer-grained probability values. For lower sampling rates like those used in the main simulations the probability axis is more poorly resolved (e.g., steps of 0.1 when 10 trials are used at each level). This inflates the choice counts in the tails of the psychometric function, with many simulated data sets containing too many values sitting on the asymptotes. This leads to steeper psychometric functions (lower noise estimates), producing average measurement noise ratios > 1.

Discussion

Manipulating the natural relationship between self-movement and image motion is a technique often used to establish basic psychophysical performance in HMDs and other settings. It reveals the relationship between estimates of audiovisual motion and idiothetic estimates of self-movement from vestibular and motor systems, as well as the underlying noise associated with each. The technique typically involves manipulating a motion-gain parameter that varies the magnitude of image motion expected from concurrent self-movement. However, as we have shown here, this can produce significant gain-dependent noise if the average self-movement varies substantially across trials. On the assumption that human observers actively compare the magnitude of self-movement to image motion, we have shown that the slope of the resulting psychometric

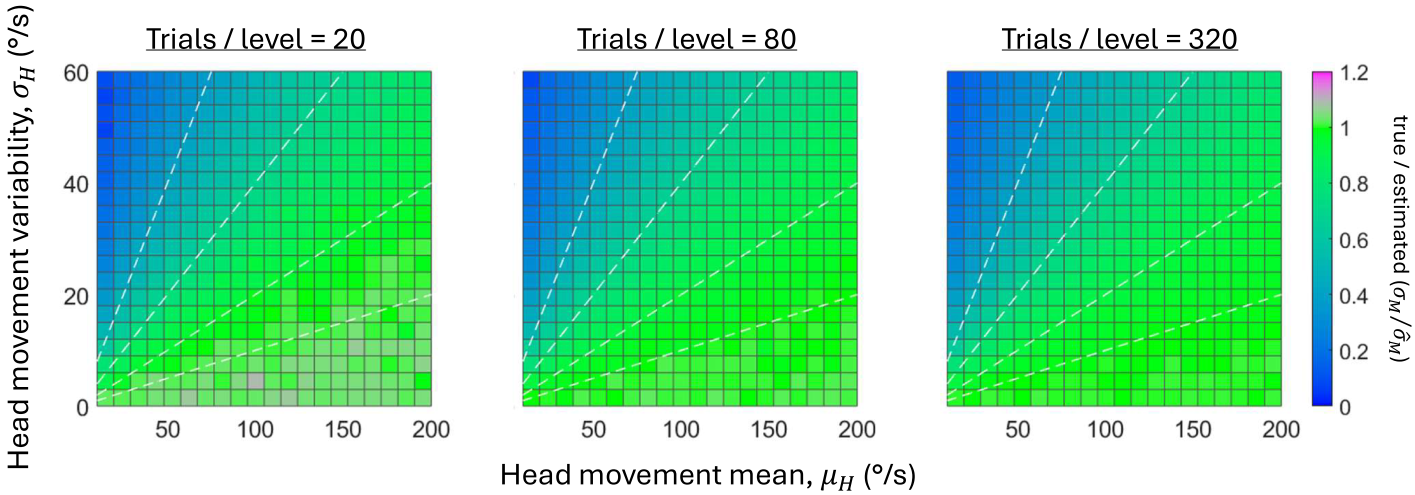

Figure 6. Measurement noise ratio obtained from simulations using a different numbers of trials per stimulus level. The model observer had high measurement noise and the cumulative Gaussian had a fixed lapse rate of 0.

function (i.e., threshold) departs significantly from a standard sigmoidal function such as a cumulative Gaussian. We used a set of simulations of a typical experiment based on a small subset of motion gains repeated a few times to reveal the areas where this is most salient. The simulations suggest the ratio of across-trial standard deviation of self-movement to its mean (the coefficient of variation, CV) can be used to identify the impact. The position of the psychometric function (i.e., the PSE) is unaffected.

The gain-dependent psychometric function derived here can be extended to other types of experiments that link display motion to self-movement, such as walking (Grechkin et al., 2016; Jaekl et al., 2005; Steinicke et al., 2008; Steinicke et al., 2009). These all invite gain-dependent noise because irrespective of the type of self-movement, or image stimulation, all psychophysical decisions rely on point estimates of relevant signals to yield ordinal judgements about a limited set of response alternatives (usually two). Hence the values used for the standard deviation and mean of head rotation in Figures 4 and 5 could be used for other types of self-movement, most easily assessed using CV. For instance, in the case of walking, one could manipulate motion gain across trials and ask observers to judge whether display motion moved “with” or “against” their self-movement (in fact, any binary decision suffices, such as whether the display moved “more” or “less” than the real self-movement). In this case, the point estimates relate to some measure of the kinematics of walking and its variability across trials.

We reiterate that the model observer makes no claims about what measures human observers use, so long as they are consistent across trials. Hence, they could use an estimate of distance or average walking speed on each trial, the peak, or the duration between steps, and so forth. What is critical is the subsequent distribution of the point estimates of these measures and their relationship to the mean (i.e., CV), not the measurements per se. In some instances, the choice of measurement may be critical for the theory being tested (for instance, whether perceived auditory motion is based on speed or displacement). In other cases, different measures may correlate well; hence, using one or other would not reflect a particular theoretical stance.

Assumptions of the gain-dependent psychometric function

We assumed that measurement noise is fixed across the range of gains used to generate the psychometric function. This means that sensory measurement noise is independent of the magnitude of the point estimate being used (e.g., rotation speed). At first sight, this seems to contradict the well-known finding that thresholds are proportional to stimulus magnitude (Weber’s Law). But, as we showed in Haynes et al. (2024), Weber’s law can still be demonstrated using this assumption, because its investigation compares conditions with quite different average stimulus magnitudes. The assumption of fixed noise across the relatively small stimulus range probed by a given psychometric function is therefore a “good enough” approximation. This is especially the case if participants are trained to perform relatively consistent self-movements within a testing block, as we did in Haynes et al. (2024). It is worth pointing out that fixed noise across the psychometric function is the (often implicit) assumption being made when fitting a single cumulative Gaussian to psychophysical data, unless the abscissa is transformed in some way (e.g. logarithmically, as in Stocker & Simoncelli, 2006). But even in the latter case, Weber's law can be accounted for in different ways, such as fixed noise combined with a non-linear change in signal mean (see Georgeson & Meese, 1996, for discussion of fixed versus variable noise).

The simulations also assumed that image and idiothetic signals had the same measurement noise for a given average head movement and variability. This is not likely to be the case because different conditions produce different degrees of external uncertainty (e.g., visual contrast or the springiness of the surface underfoot). There are many ways of manipulating external uncertainty; hence, some conditions will produce image signals with greater measurement noise than idiothetic signals and vice versa. Given we are unable to anticipate the specific conditions being addressed by a particular experiment, it seemed sensible to assume that a given combination of average head movement and variability produces the same measurement noise for each signal. We also showed the results for lower levels of measurement noise, partly because external uncertainty can vary, and partly because the estimates of image-based and idiothetic measurement noise were based on a single published study (Haynes et al, 2024).

In the case of vision, the image signal does not directly correspond to measurements of motion in the retinal image. This is because when the eyes move, display motion is not equivalent to image motion, unless a head-centred fixation point is provided (Gallagher et al., 2025; Halow, Liu, et al., 2023; Haynes et al., 2024; Hogendoorn, Alais, MacDougall, & Verstraten, 2017). The implicit assumption we made is that the observer estimates display motion regardless of how the eyes are moving; put another way, they solve the "eye-movement problem" (Warren & Hannon, 1990). There are a number of ways this can be achieved, such as using efference copy of the eye-movement command (von Holst, 1954). This would yield the information needed to make the appropriate decision in experiments that manipulate motion gain in IVEs.

Recommendations

We have shown that experiments that vary motion gain to manipulate the link between active self-movement and stimulus motion yield psychometric functions that are not always well described by a standard sigmoidal function. The extent of the problem varies with measurement noise level and the self-movement's coefficient of variation, and affects estimates of slope, not PSE. But we hasten to point out that even when a sigmoid fits the data reasonably well, this does not mean that measurement noise can be directly read from this function. Lapse rate aside, at the very least the slope of this function must be scaled by head movement mean (see Equation A6 in the Appendix). Failure to do this would mean that two observers who move their heads at different average speeds would incorrectly be considered equally sensitive if they produced identical psychometric functions.

We suggest a better strategy is to fit a gain-dependent psychometric function based on the equations derived in the Methods. This approach requires measurements of the mean of the point estimates of self-movement and their variability. In Haynes et al. (2024) and Gallagher et al. (2025), we chose to base these point estimates on the average speed per interval. Thus, for each run, we fit a Gaussian to the across-trial distribution of these point estimates to estimate μ_H and σ_H. We then used these as fixed parameters in a fitting routine that used maximum-likelihood estimation to fit the gain-dependent psychometric function to the data. We provide a downloadable MATLAB function *fitgdpmf* as an open-source fitting routine (see Methods for URL).

Keywords: motion gain, immersive virtual environments, psychometric function, external noise, psychophysics

Acknowledgments

The authors are indebted to Eugenie Lambrecht and Ann Hallemans at the Department of Rehabilitation Sciences and Physiotherapy Research Group, University of Antwerp, for providing their raw kinematic data used in Figure 3. We also thank the reviewers, whose comments led to substantial improvements to the paper.

Supported by a Leverhulme Trust project grant (RPG-2018-151).

Commercial relationships: none.
Corresponding author: Tom C. A. Freeman.
Email: freemant@cardiff.ac.uk.
Address: School of Psychology, 70 Park Place, Cardiff University, Cardiff, UK.

Footnote

[1]In Gallagher et al. (2025), the bias term was placed on the image signal not the head signal because we needed to compare differences between auditory and visual image processing via a shared head movement signal. In Haynes et al. (2024), the bias term was placed on the head-movement signal as here, but motion gain was defined with respect to a two-interval task (head-moving followed by head still). This corresponds to a world-centered gain (see final section of Methods in current article for discussion).

References

Alais, D., & Burr, D. (2004). The ventriloquist effect results from near-optimal bimodal integration. *Current Biology, 14*, 257–262.

Altman, J., & Viskov, O. (1977). Discrimination of perceived movement velocity for fused auditory image in dichotic stimulation. *The Journal of the Acoustical Society of America, 61*(3), 816–819.

Burge, J., Fowlkes, C. C., & Banks, M. S. (2010). Natural-scene statistics predict how the figure–ground cue of convexity affects human depth perception. *The Journal of Neuroscience, 30*(21), 7269–7280.

Champion, R. A., & Warren, P. A. (2017). Contrast effects on speed perception for linear and radial motion. *Vision Research, 140*, 66–72.

Chen, W., Ladeveze, N., Hu, W., Ou, S., & Bourdot, P. (2019). Comparison between the methods of adjustment and constant stimuli for the estimation of redirection detection thresholds. *International Conference on Virtual Reality and Augmented Reality* (pp. 226–245). Cham: Springer International Publishing.

De Bruyn, B., & Orban, G. A. (1988). Human velocity and direction discrimination measured with random dot patterns. *Vision Research, 28*(12), 1323–1335.

Dyde, R. T., & Harris, L. R. (2008). The influence of retinal and extra-retinal motion cues on perceived object motion during self-motion. *Journal of Vision, 8*(14), 5.1–10.

Ernst, M. O., & Banks, M. S. (2002). Humans integrate visual and haptic information in a statistically optimal fashion. *Nature, 415*, 429–433.

Fan, L., Li, H., & Shi, M. (2022). Redirected walking for exploring immersive virtual spaces with HMD: a comprehensive review and recent advances. *IEEE Transactions on Visualization and Computer Graphics, 29*(10), 4104–4123.

Freeman, T. C. A. (2001). Transducer models of head-centred motion perception. *Vision Research, 41*, 2741–2755.

Freeman, T. C. A., & Banks, M. S. (1998). Perceived head-centric speed is affected by both extra-retinal and retinal errors. *Vision Research, 38*(7), 941–945.

Freeman, T. C. A., Banks, M. S., & Crowell, J. A. (2000). Extraretinal and retinal amplitude and phase errors during Filehne illusion and path perception. *Perception & Psychophysics, 62*(5), 900–909.

Freeman, T. C. A., Champion, R. A., & Warren, P. A. (2010). A Bayesian model of perceived head-centred velocity during smooth pursuit eye movement. *Current Biology, 20*, 757–762.

Freeman, T. C. A., Culling, J. F., Akeroyd, M. A., & Brimijoin, W. O. (2017). Auditory compensation for head rotation is incomplete. *Journal of Experimental Psychology: Human Perception and Performance, 43*, 371–380, https://doi.org/10.1037/xhp0000321.

Furman, M., & Gur, M. (2012). And yet it moves: Perceptual illusions and neural mechanisms of pursuit compensation during smooth pursuit eye movements. *Neuroscience & Biobehavioral Reviews, 36*(1), 143–151.

Gallagher, M., Haynes, J. D., Culling, J. F., & Freeman, T. C. (2025). A model of audio–visual motion integration during active self-movement. *Journal of Vision, 25*(2), 8.

Garcia, S. E., Jones, P. R., Rubin, G. S., & Nardini, M. (2017). Auditory localisation biases increase with sensory uncertainty. *Scientific Reports, 7*(1), 1–10.

Garzorz, I. T., Freeman, T. C., Ernst, M. O., & MacNeilage, P. R. (2018). Insufficient compensation for self-motion during perception of object speed: The vestibular Aubert-Fleischl phenomenon. *Journal of Vision, 18*(13), 9.

Georgeson, M. A., & Meese, T. S. (2006). Fixed or variable noise in contrast discriminaition? The jury's still out.... *Vision Research, 46*, 4294–4303.

Girshick, A. R., Landy, M. S., & Simoncelli, E. P. (2011). Cardinal rules: visual orientation perception reflects knowledge of environmental statistics. *Nature Neuroscience, 14*(7), 926–932.

Grechkin, T., Thomas, J., Azmandian, M., Bolas, M., & Suma, E. (2016). Revisiting detection thresholds for redirected walking: Combining translation and curvature gains. In: *Proceedings of the ACM symposium on applied perception* (pp. 113–120).

Halow, S. J., Hamilton, A., Folmer, E., & MacNeilage, P. R. (2023). Impaired stationarity perception is associated with increased virtual reality sickness. *Journal of Vision, 23*(14), 7.

Halow, S. J., Liu, J., Folmer, E., & MacNeilage, P. R. (2023). Motor signals mediate stationarity perception. *Multisensory Research, 36*(7), 703–724.

Haynes, J. D., Gallagher, M., Culling, J. F., & Freeman, T. C. (2024). The precision of signals encoding active self-movement. *Journal of Neurophysiology, 132*(2), 389–402.

Hillis, J. M., Ernst, M. O., Banks, M. S., & Landy, M. S. (2002). Combining sensory information: Mandatory fusion within but not between senses. *Science, 298*, 1627–1630.

Hillis, J. M., Watt, S. J., Landy, M. S., & Banks, M. S. (2004). Slant from texture and disparity cues: Optimal cue combination. *Journal of Vision, 4*(12), 1.

Hogendoorn, H., Alais, D., MacDougall, H., & Verstraten, F. A. (2017). Velocity perception in a moving observer. *Vision Research, 138*, 12–17.

Jaekl, P., Jenkin, M., & Harris, L. R. (2005). Perceiving a stable world during active rotational and translational head movements. *Experimental Brain Research, 163*, 388–399.

Jones, P. R. (2016). A tutorial on cue combination and Signal Detection Theory: Using changes in sensitivity to evaluate how observers integrate sensory information. *Journal of Mathematical Psychology, 73*, 117–139.

Kerber, S., & Seeber, B. U. (2012). Sound localization in noise by normal-hearing listeners and cochlear implant users. *Ear and Hearing, 33*(4), 445–457.

Kingdom, F. A., & Prins, N. (2016). *Psychophysics: A proctical Introduction*. New York: Academic Press.

Kruse, L., Langbehn, E., & Steinicke, F. (2018). I can see on my feet while walking: Sensitivity to translation gains with visible feet. In: *2018 IEEE conference on virtual reality and 3D user interfaces (VR)* (pp. 305–312). Piscataway, NJ: IEEE.

Lambrecht, E., Struye, J., Beckwée, D., Vereeck, L., De Hertogh, W., Embrechts, E., . . . Hallemans, A. (2025). Standardizing head movements in gait assessment through augmented reality, a cross-sectional study. *Gait & Posture, 122*, 292–299.

Laming, D. (2009). Weber's law. In *Inside Psychology: A science over 50 years* (pp. 179–191). London: Oxford University Press.

Landy, M. S., Maloney, L. T., Johnston, E. B., & Young, M. (1995). Measurement and modelling of depth cue combination: in defense of weak fusion. *Vision Research, 35*(3), 389–412.

MacLellan, M. J., & Patla, A. E. (2006). Adaptations of walking pattern on a compliant surface to regulate dynamic stability. *Experimental Brain Research, 173*, 521–530.

MacNeilage, P. R., Banks, M. S., Berger, D. R., & Bulthoff, H. H. (2007). A Bayesian model of the disambiguation of gravitoinertial force by visual cues. *Experimental Brain Research, 179*, 263–290.

Mallery, R. M., Olomu, O. U., Uchanski, R. M., Militchin, V. A., & Hullar, T. E. (2010). Human discrimination of rotational velocities. *Experimental Brain Research, 204*, 11–20.

Mamassian, P., Landy, M. S., & Maloney, L. T. (2002). Bayesian modelling of visual perception. In: *Probabilistic models of the brain: Perception and neural function* (pp. 13–36). Cambridge, MA: The MIT Press.

Moroz, M., Garzorz, I., Folmer, E., & MacNeilage, P. (2019). Sensitivity to visual speed modulation in head-mounted displays depends on fixation. *Displays, 58*, 12–19.

Nilsson, N. C., Peck, T., Bruder, G., Hodgson, E., Serafin, S., Whitton, M., . . . Rosenberg, E. S. (2018). 15 years of research on redirected walking in immersive virtual environments. *IEEE Computer Graphics and Applications, 38*(2), 44–56.

Nilsson, N. C., Suma, E., Nordahl, R., Bolas, M., & Serafin, S. (2016). Estimation of detection thresholds for audiovisual rotation gains. In: *2016 IEEE Virtual Reality (VR)* (pp. 241–242). Piscataway, NJ: IEEE.

Oruç, I., Maloney, L. T., & Landy, M. S. (2003). Weighted linear cue combination with possibly correlated error. *Vision Research, 43*(23), 2451–2468.

Powell, G., Meredith, Z., McMillin, R., & Freeman, T. C. A. (2016). Bayesian models of individual differences: Combining autistic traits and sensory thresholds to predict motion perception. *Psychological Science, 27*(12), 1562–1572.

Prins, N. (2019). Too much model, too little data: How a maximum-likelihood fit of a psychometric function may fail, and how to detect and avoid this. *Attention, Perception, & Psychophysics, 81*(5), 1725–1739.

Prins, N., & Kingdom, F. A. (2018). Applying the model-comparison approach to test specific research hypotheses in psychophysical research using the Palamedes toolbox. *Frontiers in Psychology, 9*, 1250.

Razzaque, S., Swapp, D., Slater, M., Whitton, M. C., & Steed, A. (2002). Redirected walking in place. *Egve, 2*, 123–130.

Scarfe, P. (2022). Experimentally disambiguating models of sensory cue integration. *Journal of Vision, 22*(1), 5.

Serafin, S., Nilsson, N. C., Sikstrom, E., De Goetzen, A., & Nordahl, R. (2013). Estimation of detection thresholds for acoustic based redirected walking techniques. In: *2013 IEEE Virtual Reality (VR)* (pp. 161–162). Piscataway, NJ: IEEE.

Sotiropoulos, G., Seitz, A. R., & Seriés, P. (2014). Contrast dependency and prior expectations in human speed perception. *Vision Research, 97*, 16–23, https://doi.org/10.1016/j.visres.2014.01.012.

Souman, J. L., Hooge, I. T. C., & Wertheim, A. H. (2006). Frame of reference transformations in motion perception during smooth pursuit eye movement. *Journal of Computational Neuroscience, 20*(1), 61–76.

Steinicke, F., Bruder, G., Jerald, J., Frenz, H., & Lappe, M. (2008). Analyses of human sensitivity to redirected walking. In: *Proceedings of the 2008 ACM symposium on Virtual reality software and technology* (pp. 149–156).

Steinicke, F., Bruder, G., Jerald, J., Frenz, H., & Lappe, M. (2009). Estimation of detection thresholds for redirected walking techniques. *IEEE Transactions on Visualization and Computer Graphics, 16*(1), 17–27.

Stocker, A. A., & Simoncelli, E. P. (2006). Noise characteristics and prior expectation in human visual speed perception. *Nature Neuroscience, 9*(4), 578–585.

Teng, X., Allison, R. S., & Wilcox, L. M. (2023). Manipulation of motion parallax gain distorts perceived distance and object depth in virtual reality. In: *2023 IEEE Conference Virtual Reality and 3D User Interfaces (VR)* (pp. 398–408). Piscataway, NJ: IEEE.

Thompson, P. (1982). Perceived rate of movement depends on contrast. *Vision Research, 22*(3), 377–380.

von Holst, E. (1954). Relations between the central nervous system and the peripheral organs. *British Journal of Animal Behaviour, 2*, 89–94.

Warren, W. H., & Hannon, D. J. (1990). Eye movements and optical flow. *Journal of the Optical Society of America A, 7*(1), 160–169.

Wei, X.-X., & Stocker, A. A. (2015). A Bayesian observer model constrained by efficient coding can explain "anti-Bayesian" percepts. *Nature Neuroscience, 18*(10), 1509.

Wertheim, A. H. (1994). Motion perception during self-motion - the direct versus inferential controversy revisited. *Behavioral and Brain Sciences, 17*(2), 293–311.

Wichmann, F. A., & Hill, N. J. (2001). The psychometric function: I. Fitting, sampling, and goodness of fit. *Perception & Psychophysics, 63*(8), 1293.

Williams, N. L., & Peck, T. C. (2019). Estimation of rotation gain thresholds considering fov, gender, and distractors. *IEEE Transactions on Visualization and Computer Graphics, 25*(11), 3158–3168.

Xu, Z.-X., & DeAngelis, G. C. (2025). Seeing a three-dimensional world in motion: How the brain computes object motion and depth during self-motion. *Annual Review of Vision Science, 11*, 423–446.

Appendix: Comparing true to estimated measurement noise

Slope of gain-dependent psychometric function at PSE

The derivative of Equation 11 with respect to g is:

$$\frac{dP}{dg} = (1-\lambda)\,\Phi\left(d'\right) \cdot \frac{d}{dg}\left[d'(g)\right] \quad \text{(A1)}$$

where $\Phi(d')$ is the integrand in Equation 12, and $\frac{d}{dg}[d'(g)]$ can be found using the chain rule:

$$\frac{d}{dg}\left[d'(g)\right] = -\mu_H \frac{\sigma_h^2 + \sigma_i^2}{\left((b-g)^2\sigma_H^2 + \sigma_h^2 + \sigma_i^2\right)^{\frac{3}{2}}} \quad \text{(A2)}$$

At the PSE, $d' = \mu_m = 0$; thus $g = b$. Substituting for these values in Equation A1:

$$\frac{dP}{dg} = (1-\lambda)\Phi(0) \cdot \frac{d}{dg}[d'(b)] = -\frac{(1-\lambda)\mu_H}{\sqrt{2\pi\left(\sigma_h^2 + \sigma_i^2\right)}} \quad \text{(A3)}$$

Why the slope is negative is explained in the Methods (section "IVE gain versus world gain").

Slope of best-fitting cumulative Gaussian at PSE

Kingdom and Prins (2016, chapter 4) define the cumulative Gaussian used by the Palamedes toolbox as:

$$\Phi(x) = \frac{\beta}{\sqrt{2\pi}} \int_{-\infty}^{x} e^{-\beta^2(x-\alpha)^2}/2\, dx \quad \text{(A4)}$$

At the PSE, $x = \alpha$. Including a lapse rate, the derivative with respect to x is:

$$\frac{d}{dx}\left[\Phi(\alpha)\right] = \frac{(1-\lambda)\,\beta}{\sqrt{2\pi}} \quad \text{(A5)}$$

Best estimate of noise

Equation A3 shows that measurement noise alone determines the slope of the gain-dependent psychometric function *at the PSE*: gain-dependent noise only affects its shape either side. Put another way, the same slope would be obtained for a model observer with or without gain-dependent noise. This fact allows us to determine the best estimate of true measurement noise that can be achieved when fitting a single cumulative Gaussian. Comparing Equation A3 and Equation A5, it must be that case that:

$$\beta = \frac{\mu_H}{\hat{\sigma}_M} \quad \text{(A6)}$$

where $\hat{\sigma}_M$ is the best estimate of the true measurement noise $\sigma_M = \sqrt{(\sigma_h^2 + \sigma_i^2)}$. Hence, the ratio of true measurement noise to best estimate is given by:

$$\frac{\sigma_M}{\hat{\sigma}_M} = \frac{\beta\sqrt{\left(\sigma_h^2 + \sigma_i^2\right)}}{\mu_H} \quad \text{(A7)}$$

Note this is not that dissimilar to taking the ratio of slopes, which would scale $\frac{\sigma_M}{\hat{\sigma}_M}$ by the ratio of $(1-\lambda)$ in Equations A3 and A5.